


Arterial-Friendly Local Ramp Metering Control Strategy

Yao Cheng¹ and Gang-Len Chang¹

Transportation Research Record
2021, Vol. 2675(7) 67–80
© National Academy of Sciences:
Transportation Research Board 2021
Article reuse guidelines:
sagepub.com/journals-permissions
DOI: 10.1177/0361198121994581
journals.sagepub.com/home/trr
 SAGE

Abstract

To prevent local streets being blocked by overflowing on-ramp queues, a standard practice of ramp metering control is to restrain its function when a series of preset conditions are identified by on-ramp queue detectors. Such a trade-off between potential ramp queue spillback and the restraint resulting from the operation of metering control may often fail to either effectively mitigate bottlenecks caused by on-ramp waving or convince arterial users and local traffic agencies of the need for ramp metering operations. This study, therefore, presents an arterial-friendly local ramp metering system (named AF-ramp) that can achieve the target metering rate to produce optimal freeway conditions without ramp queues spilling back onto local streets. This is achieved by concurrently optimizing the signal plans for those intersections that send turning flows to the ramp. At this stage, this system has been developed for time-of-day control. It could also serve as the base module for extending to real-time control, or multi-ramp coordinated operations. The AF-ramp model, with its ability to optimize the arterial signals concurrently with the ramp metering rate, can ensure the best use of the capacity of local intersections and prevent any gridlock caused by overflows from on-ramp queue spillback or arterial turning traffic. With extensive simulation experiments, the evaluation results confirmed the AF-ramp model's effectiveness in improving traffic conditions on both the freeway and its neighboring arterial links at the same time. This study has also introduced the real-time extension of the proposed model and a framework of a transition from the time-of-day control to fully responsive real-time operations.

Implementing ramp metering control has long been recognized as a strategy that can be effective in improving traffic efficiency along congested freeway segments. Control functions, such as a signal to regulate on-ramp vehicle flows, are used to break up arriving platoons to smooth the traffic flow merging onto the freeway and to prevent the likely formation of freeway bottlenecks.

Depending on the availability of real-time information, a local ramp metering control system can be operated under a pre-timed (1–3) or a traffic-responsive mode (4–9). As one of the pioneer studies on pre-timed ramp metering, Wattleworth (1) generates optimized metering rates with linear programming under the constraints of freeway mainline capacity with the objective of maximizing the total volume of traffic joining the freeway. Using detectors to measure the occupancy rate, ALINEA (4) determines the ramp metering rate based on the difference between a preset and the observed occupancies. Various extensions along the core concept of ALINEA have been proposed in the literature to use flow information instead of occupancy, and to take into account the traffic state on the upstream and downstream segments. (6)

Over the past two decades, traffic control researchers have also extended local metering operations to

coordinated control of multiple ramps along the congested freeway segments. For example, SystemWide Adaptive Ramp Metering (SWARM) (10) computes a coordinated metering rate based on the estimated density and a preset local rate using distance headway measurements, and then selects the more restrictive one. In HEuristic Ramp metering coOrdination (HERO) (11), each on-ramp is independently controlled with ALINEA while all ramps are connected to each other through a central controller so that a master ramp, where the bottleneck occurs, can be identified and then given priority during coordinated control. METALINE (12) determines the metering rates at different on-ramps using a list of occupancy values from several detectors. This has been reported to yield an increase in the mainline speed in several cities. Essentially, coordinated ramp metering strategies usually use the available space at upstream on-ramps so that the metered vehicles can be stored in an

¹Department of Civil & Environmental Engineering, University of Maryland, College Park, MD

Corresponding Author:

Yao Cheng, chengyao09@gmail.com

expanded space to avoid the formation of bottlenecks. Other examples of coordinated ramp control strategies include systematic control with linear programming (1), AIMD (13), HELPER (14), and the Advanced Real-time Metering System (ARMS) (15).

However, despite the abundance of literature in freeway ramp metering, such strategies, either at local or coordinated levels, often favor the operation of the freeway but do not account for their potential negative impact on the local traffic caused by the excessive on-ramp queues. For example, while performing well in maintaining a desirable flow rate on the freeway, ALINEA (4) and the Neural control algorithm (9) may create long queues at the on-ramp (16, 17). Such long queues created by ramp control often result in blockage of the arterial's signal and an increase in vehicle emissions on the on-ramps (18). A standard practice for circumventing the queue spillback issue is to restrict the metering rate when a deployed ramp queue detector identifies a high occupancy rate (10, 11, 19) or when the ramp entering volume is over the preset level (6, 20). Kattan and Saidi (18) further accounted for the on-ramp queue length in the optimization of the ramp metering rate by integrating the ramp waiting time in the objective function. However, since ramp metering control is primarily deployed at those interchanges experiencing high on-ramp volumes, the resulting on-ramp queue length is likely to trigger frequent overriding calls by the queue detectors, thus rendering it difficult to achieve the desired level of performance.

As is well recognized in the traffic control community, excessive ramp waiting times and the resulting queue spillbacks to the connected surface streets are two significant concerns frequently raised by both the users of local arterials and the agencies responsible for traffic control and management. Most existing practices seek only to optimize the activation and rates of ramp metering, and thus cannot, even taking the on-ramp queue length into consideration, effectively address such concerns. Furthermore, a ramp control system may not help the target freeway segment operate at peak efficiency if it suffers from frequent override activations caused by potential on-ramp queue spillover to the local arterial.

An alternative methodology for ramp metering proposed in this study is to expand the control area to include not only the interchange's on-ramp freeway segment but also all local intersections feeding traffic flows to the on-ramp (see Figure 1). Thus, the control strategies will aim to achieve concurrent optimization of both the ramp metering rate and the signal plans for all intersections within the control area so that both the local freeway and arterial segments can simultaneously achieve their optimal state under the given volumes and available roadway capacity.

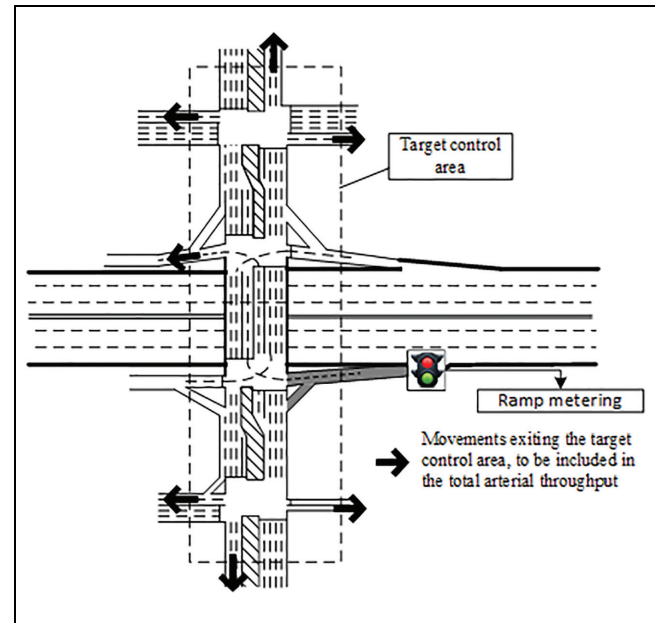


Figure 1. Control area of the proposed arterial-friendly local ramp metering strategy.

Under such a design notion, the control objective for the local ramp metering to optimize the selected measure of effectiveness (MOE) ought to cover not only the freeway and the on-ramp, but also all arterial intersections, either feeding traffic to the ramp or likely to suffer from excessive ramp queues. Such an integrated ramp metering control strategy, accounting for traffic conditions both on the on-ramp and at local intersections, has not been extensively studied in the literature. Su et al. (21) proposed a coordinated control strategy for an on-ramp and its feeding intersections but optimized the metering rate and intersection signals in sequential steps to favor mainly the freeway operations. More specifically, a control system intending to achieve the target metering rate to optimize the freeway conditions but not to spill ramp queues back to the surface street, should simultaneously optimize the signal plans, including the phase sequences and offsets for those intersections sending turning flows to the ramp, so that flows arriving at the ramp can be regulated effectively by the signals, thus preventing potential arterial gridlocks caused by overflows of turning traffic with path-flow-based progression. Such an arterial-friendly ramp control system will be more likely to ease the concerns of local commuters and offer the best prospect for comprehensive field implementation at local freeway bottlenecks caused mainly by heavy on-ramp weaving flows.

With such a control objective in mind, this study presents an arterial-friendly local ramp metering system (named AF-ramp) for time-of-day control. The proposed system can also serve as the base module for an

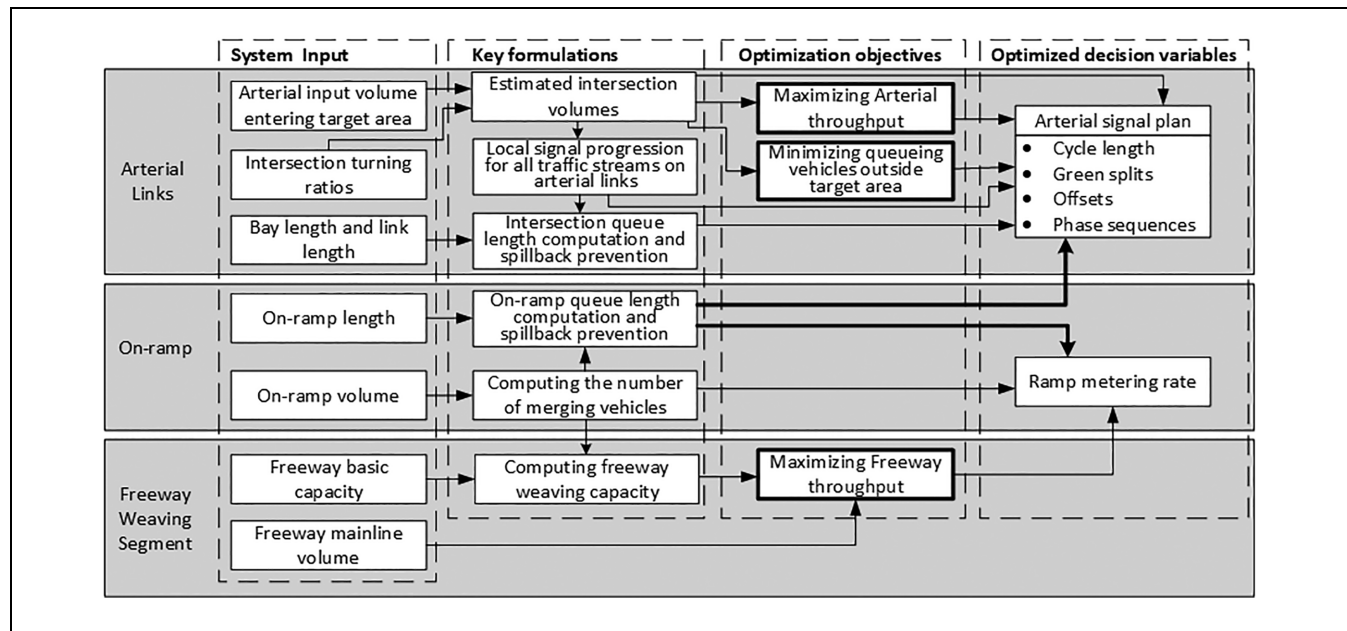


Figure 2. Model structure for the arterial-friendly local ramp metering control system.

extension to real-time on-line control, or multi-ramp coordinated operations under a reliable traffic surveillance environment. Figure 2 shows the principal modules and their interrelations within the proposed AF-ramp system, including the control objectives and model output. Its key system features, as illustrated in the figure, include its ability to:

- maximize the total throughput for both the freeway and arterial links within the control area;
- prevent ramp queues from spilling back to neighboring local streets by coordinating intersection signal plans with ramp metering control;
- minimize the impact of an intersection's turning-to-ramp flows on the arterial's other traffic flow movements with local progression, using a set of specially designed offsets to provide progression for all path flows within the control area of the local arterial; and
- optimize the signal plan, including the phase sequences, for each intersection to ensure that its turning queues heading to the on-ramp will not exceed the available bay length.

A detailed discussion of mathematical formulations to model those key system features and operational constraints is presented below, followed by performance evaluation with extensive numerical analyses and simulation experiments.

Model Formulations

To facilitate the presentation of the proposed system's embedded formulations, Table 1 lists the key notations of all variables and parameters used in this study.

Available Capacity to Accommodate the On-Ramp Flows

The optimal on-ramp metering rate, regardless of the control strategy, depends primarily on the receiving freeway segment's available capacity. The capacity, however, is not a constant but a variable that is a function of mainline and ramp volumes, freeway geometric features, the composition of traffic flows, and the weaving behaviors of the driving populations. However, from the perspective of developing control strategies, it is recognized that such a capacity drop mainly varies with two variables of arriving flow rates: those from the ramp's upstream mainline segments; and those from the connected local intersections. Because of the need to exercise corporative deceleration for on-ramp flows, traffic streams on the freeway mainline, especially in the rightmost lane, often comprise a series of voids between a leading on-ramp and following mainline vehicles. Such voids, as noted by Lertworawanich and Elefteriadou (22) and Won (23), inevitably contribute to a reduction in the freeway segment's available capacity to accommodate the on-ramp traffic.

Conceivably, depending on the purpose of having such capacity reduction information (e.g., service quality

Table 1. List of Key Notations

Sets	
Ω	Set of intersection movements heading to the on-ramp
Δ	Set of movements exiting the target network
Φ	Set of movements entering the target network
Parameters	
v_i	Average vehicle speed on Lane i of the freeway (fps)
a	Deceleration rate of the rear vehicle for cooperative lane change (ft/s ²)
k_i	Average density on Lane n of the freeway (vpm)
C_w	Capacity in the weaving section (vph)
C_b	Freeway basic capacity (vph)
l	Average vehicle spatial headway (ft)
L_o	On-ramp length (veh)
s_o	Saturation flow rate at the ramp metering point (vph)
$d(m), u(m)$	Downstream and upstream movements of traffic path m between two adjacent intersections
t_i	Travel time from intersection i to $i + 1$ (in cycle);
$V_{\mu,i}$	Volume demand for movement μ at intersection i (vph)
V_{fm}	Freeway mainline demand (vph);
$f_{\mu,i}$	Lane-use factor based on the number of lanes for movement μ at intersection i
$r_{\mu,i}$	Volume ratio of movement μ from arterial at intersection i
$L_{b,i}, L_{l,i}$	Bay length and the link length at intersection i (veh)
t_l	Lost time for each signal phase (s)
T	Time duration of the study (h)
C_{max}, C_{min}	Upper bound and lower bound for the cycle length (s)
δ_1, δ_2	Parameters for estimating the weaving section capacity
γ	Robustness factor that represents the sensitivity of volume fluctuation to the occurrence of queue spillback
α, β	Weighting factors in the objective function
Variables	
r_o	On-ramp metering green ratio
C_{r1}	Capacity reduction in the weaving section because of the cooperative deceleration of the mainline vehicle behind the merging vehicle (vph)
C_{r2}	Capacity reduction in the weaving section because of pre-allocation lane change (vph)
V_o^a	Number of on-ramp vehicles merging into the freeway mainline (veh)
$V_{\mu,i}^a$	Actual volume for movement μ at intersection i (vph)
V_f^a	Freeway throughput (vph)
V_r^a	Arterial throughput (vph)
R_i	Number of queueing vehicles outside the target area because of the limited green time (vph)
L_{rv}	The length of the rear void created by cooperative deceleration of the freeway mainline vehicle behind the on-ramp merging vehicle (ft)
l_p	Queue length caused by excessive demand at the end of the study period (veh)
l_c	Queue length caused by arrivals from the upstream intersection in every cycle (veh)
ξ	Reciprocal of the cycle length at the arterial intersections (1/s)
$b_{m,i}$	Local progression bands, that is, the duration within which vehicles from traffic path m can traverse intersections $i-1$ and i without stop (in cycle)
$t_{\mu,i}^a, t_{\mu,i}^b$	Start and end of the green phase for downstream movement μ at intersection i
$\tau_{d(m),i}$	Queue clearance time of movement $d(m)$ at intersection i (in cycle)
$l_{\mu,i}$	Queue length for movement μ at intersection i (veh)
$g_{\mu,i}$	Green ratio, including the lost time (in cycle)
$g_{t,i}(\bar{g}_{t,i})$	Through green ratio for outbound (inbound) direction along the arterial (in cycle)
$g_{l,i}(\bar{g}_{l,i})$	Left-turn green ratio for outbound (inbound) direction from the arterial (in cycle)
$g_{ml,i}(\bar{g}_{ml,i})$	Green ratio for side street left-turn that would join outbound (inbound) direction along the arterial (in cycle)
$g_{mt,i}(\bar{g}_{mt,i})$	Through green ratio for side street where the corresponding left-turn would join outbound (inbound) direction along the arterial (in cycle)

Note: fps = feet per second; vph = vehicles per hour; vpm = vehicles per mile; veh = vehicles.

evaluation or adaptive on-line control) and its required accuracy, one can perform such an estimation from either the macroscopic or microscopic perspective, based on some or all of the following data: geometric features of

freeway and ramps; traffic flow characteristics; volume distributions across lanes; behavioral patterns of the driving populations; and the percentage of heavy vehicles (24–26). Therefore, in seeking to design time-of-day local

ramp control, this study employs the following equation to approximate the capacity reduction because of the total loss time incurred by those voids between mainline and ramp vehicles:

$$L_{rv} = \frac{v_1^2 - v_0^2}{2a} \quad (1)$$

$$C_{r1} = \delta_1 V_o^a \frac{v_1^2 - v_0^2}{2al} \quad (2)$$

where

L_{rv} is the length of the rear void (ft),

v_1 and v_0 refer to the vehicle speed in the rightmost and acceleration lanes (ft/s), respectively, and

a denotes the deceleration rate of the rear vehicles following the on-ramp flows (ft/s²).

Therefore, L_{rv} divided by the vehicle length l , offers the base for approximating the impact of per void created by on-ramp vehicles. One can then approximate the resulting reduction in freeway capacity because of on-ramp volume V_o^a , as C_{r1} , where δ_1 is a parameter. Note that the magnitude of capacity reduction identified with Equation 2 would be more prominent under high mainline volume scenarios, where spaces between vehicles are limited.

Equation 3 shows that the allowable on-ramp volume can be determined by the actual flow rate for movement μ at intersection i , the set of movements heading to the on-ramp (Ω), the on-ramp metering green ratio (r_o), and the saturation flow rate (s_o) for the metered on-ramp.

$$V_o^a = \min \left(s_o r_o, \sum_{\mu \in \Omega} V_{\mu,i}^a \right) \quad (3)$$

Note that the collective manifestation of ramp upstream drivers' discretionary lane-changing maneuvers to avoid the speed impedance by ramp flows, as noted by Kwon (27), may also contribute significantly to the capacity reduction of the downstream freeway segment. Methodologies for a precise estimate of such a lane-changing frequency and the resulting impacts on the capacity from a behavioral perspective are available elsewhere (28–30), but for the purpose of this application it is assumed to be a function of the density ratio between the rightmost lane (i.e., lane 1) and its neighboring lane (lane 2), as expressed below:

$$C_{r2} = \delta_2 V_o^a \frac{k_2}{k_1 + k_2} \quad (4)$$

where k_1 and k_2 denote, respectively, the densities for lane 1 and lane 2 before receiving the on-ramp merging vehicles (vehicles per mile), and δ_2 is a parameter.

Note that Equation 4 is grounded in the assumption that the density ratio between lane 1 and lane 2, before

and after receiving the merging flows, will be approximately unchanged, because traffic flows, when perceiving the impacts from on-ramp flows, tends to evolve to the same state by exercising discretionary lane changes. Therefore, to achieve such a state after accommodating on-ramp volumes, if without those upstream lane changes, it is expected that the $k_2/(k_1 + k_2)$ ratio of total on-ramp volume should be distributed to lane 2. However, most such on-ramp vehicles, as shown in most field observations, tend to stay in lane 1 over certain time intervals, thus often triggering a series of lane changes by those upstream lane-1 vehicles so that the lane density ratio between these two neighboring lanes can evolve back to the same level at the downstream segment of the on-ramp. Each such lane-changing maneuver, approximated with the number of on-ramp vehicles to be distributed to lane 2 to maintain the pre-merge density ratio, will occupy the space in both lane 1 and lane 2, thus inevitably impeding the traffic flow and consequently contributing to the capacity reduction, denoted as C_{r2} , on the downstream segment.

As such, the available freeway capacity for local ramp control, accounting for the aforementioned two primary impacts, can be expressed as follows:

$$C_w = C_b - C_{r1} - C_{r2} = C_b - \delta_1 V_o^a \frac{v_1^2 - v_0^2}{2al} - \delta_2 V_o^a \frac{k_2}{k_1 + k_2} \quad (5)$$

Constraints for Ramp Queues

The on-ramp queue length typically consists of the residual queues after the whole control period and the arriving vehicles discharged per cycle from connected intersections. For the former, one can formulate Equation 6 to compute the resulting queue length (in the unit of vehicles), whereas the latter can be approximated with Equation 7. During the target control period, the total queue length is constrained to be within the ramp length, as specified by Equation 8.

$$l_p = \max \left(\sum_{\mu \in \Omega} V_{\mu,i}^a - s_o r_o, 0 \right) \times T \quad (6)$$

$$l_c = \sum_{\mu \in \Omega} V_{\mu}^a / 3600\xi \quad (7)$$

$$l_p + l_c \leq L_o \quad (8)$$

where l_p represents the queue length (number of vehicles [veh]) because of the excessive demand at the end of each control period, and l_c reflects the queue length (veh) of arriving vehicles per cycle from connected intersections.

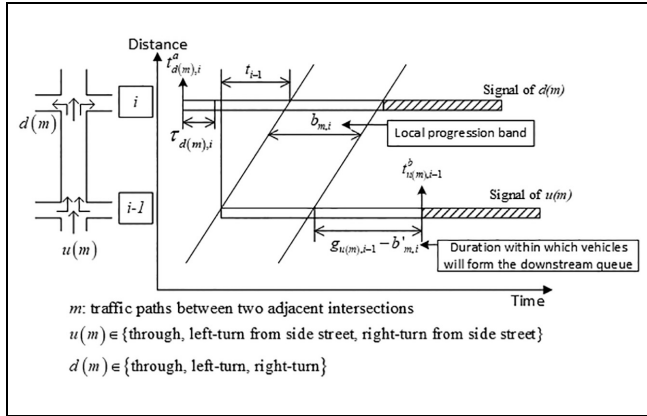


Figure 3. Example of a local progression band for one traffic path between two adjacent intersections.

Formulations of Intersection Queue Constraints

To ensure that the proposed ramp control will not cause queue spillback at those intersections feeding flows to the freeway, the proposed system has adopted the local band notion (31) to estimate the number of vehicles stopping at the intersections within the ramp's affected area. Figure 3 illustrates the local band for one traffic path between two adjacent intersections in the time-space diagram, where a specially designed signal plan, coordinated with ramp control, is included in the proposed system to offer a progression band for each of those nine possible path flows over the arterial link between two intersections in the vicinity of an interchange. Note that each of those nine possible path flows consists of one upstream movement $u(m)$ and one downstream movement $d(m)$, as shown in Figure 3. Only vehicles not within their local progression bands have to stop at the downstream intersection and contribute to the queues.

A mathematical expression for such local progression bands for the outbound direction is shown with Equation 9:

$$b_{m,i} = \min(t_{d(m),i}^b, t_{u(m),i-1}^b + t_{i-1}) - \max(t_{d(m),i}^a + \tau_{d(m),i}, t_{u(m),i-1}^a + t_{i-1}) \quad (9)$$

where

$b_{m,i}$ is progression band for vehicles from path flows m to move from intersections $i-1$ to i ,

$d(m)$ and $u(m)$ are the downstream and upstream movements for traffic path-flow m ,

$\tau_{d(m),i}$ is the queue clearance time of movement $d(m)$ at intersection i (in cycle),

t_i is the travel time from intersection i to $i+1$ (in cycle),

$t_{d(m),i}^a$ and $t_{d(m),i}^b$ are the start and end of the green phase for downstream movement m at intersection i , respectively; and

$t_{u(m),i}^a$ and $t_{u(m),i}^b$ are the start and end of the green phase for upstream movements m at intersection i , respectively.

Note that the second term on the right-hand side, $\max(t_{d(m),i}^a + \tau_{d(m),i}, t_{u(m),i-1}^a + t_{i-1})$, shows the starting time of the local progression band, which is to be determined by the arrival time of the first vehicle from traffic path m to the downstream intersection and the queue clearance time of the downstream movement associated with traffic path m . By the same token, the ending time of the local progression band, denoted by $\min(t_{d(m),i}^b, t_{u(m),i-1}^b + t_{i-1})$, depends on the earlier time between the end of the downstream green phase and the last vehicle arrival from the same traffic path to the downstream intersection.

From the local bands associated with left-turn and through movements at the downstream intersection, one can formulate their resulting queues at the onset of the green phase at the downstream intersection based on their volumes and turning ratios, as follows:

$$l_{\mu,i} = \sum_{d(m)=\mu} V_{u(m),i-1}^a r_{d(m),i} (g_{u(m),i-1} - b_{m,i-1}) f_{d(m),i} / 3600\xi, \quad (10)$$

$\mu = \text{through or left-turn}$

where

$l_{\mu,i}$ denotes the queue length for movement μ at intersection i (veh),

$f_{d(m),i}$ refers to the lane-use factor based on the number of lanes for movement $d(m)$ at intersection i , and

$r_{d(m),i}$ is the volume ratio of movement $d(m)$ from arterial at intersection i .

Therefore, to prevent the queue spillback from the left-turn bay and the through lanes, one can present the following equations:

$$l_{\mu,i} \frac{s}{s - V_{\mu,i} f_{\mu,i}} \times \gamma \leq L_{b,i} \quad (11)$$

$$l_{\mu,i} \frac{s}{s - V_{\mu,i} f_{\mu,i}} \times \gamma \leq L_{l,i} \quad (12)$$

where

s is the saturation flow rate (vehicles per hour [vph]),

$L_{b,i}$ and $L_{l,i}$ are the bay length and the link length at intersection i , respectively (veh), and

γ is a robustness factor greater or equal to 1 that represents the sensitivity of volume fluctuation to the occurrence of queue spillback.

The left-hand side represents the estimated maximum queue length during a cycle. The queue discharging time in Equation 9 can then be estimated with the obtained queue length as follows:

$$\tau_{\mu,i} = I_{\mu,i} \frac{3600\xi}{s - V_{\mu,i}f_{\mu,i}} \quad (13)$$

Following the same logic, one can develop similar constraints as Equations 9–13 for the inbound direction.

Constraints for Intersection Flows and Signal Parameters

Note that the actual number of vehicles arriving at a downstream intersection can be derived from the flows moving out from its upstream intersection, as with Equation 14.

$$V_{\mu,i}^a = r_{\mu,i} \sum_{d(m)=\mu} V_{u(m),i-1}^a \quad (14)$$

If an internal link within the target area experiences overflow, the queues would rapidly spill back to the upstream intersection and cause a local bottleneck. Such a situation can be avoided by providing sufficient green time to discharge all vehicles on the links within the target control area, as shown in Equation 15.

$$V_{\mu,i}^a f_{\mu,i} \leq (g_{\mu,i} - t_l \xi) s \quad (15)$$

where $g_{\mu,i}$ represents the green ratio, including the lost time (in cycle), and t_l denotes the lost time (s). The green ratios at the intersections should satisfy the following constraints to be practical:

$$g_{t,i} + \bar{g}_{t,i} = g_{l,i} + \bar{g}_{l,i} = g_{major,i} \quad (16)$$

$$g_{mt,i} + \bar{g}_{ml,i} = g_{ml,i} + \bar{g}_{mt,i} = g_{minor,i} \quad (17)$$

$$g_{major,i} + g_{minor,i} = 1 \quad (18)$$

The cycle length will be constrained with its lower and upper bounds using Equation 19.

$$1/C_{\max} \leq \xi \leq 1/C_{\min} \quad (19)$$

Objective Function

As mentioned above, this study focuses on maximizing the total throughput for the freeway and the local arterial. Furthermore, queueing vehicles that may not be able to enter the control area because of the lower cycle length and green ratio, should cause a penalty in the objective function since these vehicles would incur excessive delay if not properly discharged. The objective function of the proposed model can, therefore, be expressed as:

$$\text{Max } V_f^a + \alpha V_r^a - \beta \sum_i R_i \quad (20)$$

$$V_f^a = \min(V_{fm} + V_o, C_w) \quad (21)$$

$$V_r^a = \sum_i \sum_{\mu \in \Delta} V_{\mu,i}^a \quad (22)$$

$$R_i = \sum_{\mu \in \Phi_i} (V_{\mu,i} - V_{\mu,i}^a) \quad (23)$$

where

V_f^a denotes freeway throughput (vph), which is determined by freeway mainline demand, on-ramp volume, and weaving section capacity, as expressed in Equation 21,

V_r^a represents the arterial throughput (vph), which counts all vehicles exiting the target area, as expressed in Equation 22,

R_i is the number of queueing vehicles outside the target area because of the limited green time on the entering approaches of intersection i (vph),

α and β are weighting factors,

V_{fm} denotes the freeway mainline demand (vph),

$V_{\mu,i}$ is the volume demand for movement μ at intersection i (vph),

Δ is the set of movements exiting the target network, and Φ_i is the set of movements entering the target network at intersection i .

In brief, the proposed model can be formulated with Mixed Integer Linear Programming (MILP) and can be summarized as follows:

$$\text{Max } V_f^a + \alpha V_r^a - \beta \sum_i R_i$$

s.t.

Equations 21–23

Freeway capacity constraints: Equations 2–5

On-ramp queue constraints: Equations 6–8

Intersection queue constraints: Equations 9–13

Constraints for intersection flows and signal parameters: Equations 14–19

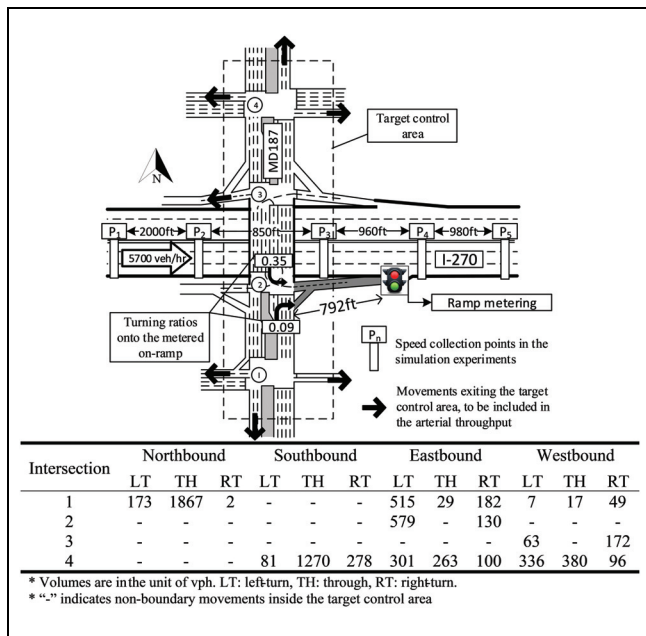
Case Study

To verify the unique capability of the developed AF-ramp model and evaluate its effectiveness, this case study has included both numerical investigations and simulation experiments within a real-world network. The numerical results are presented to show the proposed model's functions in response to the volume surge and geometric constraints such as the ramp length, while the resulting MOEs and the impacts on the local arterial under such control are assessed with microscopic traffic simulation. All analysis results from this case study constitute the basis to confirm the AF-ramp model's foremost function of concurrently improving traffic conditions on the freeway and local arterials, but not causing queues to overflow from the on-ramp.

Table 2. Optimization Results from the Proposed Model under Four Designed Scenarios

	Scenario 1	Scenario 2	Scenario 3	Scenario 4
Ramp metering green ratio	0.38	0.42	0.47	0.45
Arterial cycle length (s)	90	90	150	100
SB LT green ratio at Intersection 2	0.36	0.40	0.42	0.41
Intersection offsets (s)				
Intersection 1	0	12	135	0
Intersection 2	83	70	101	59
Intersection 3	84	0	3	35
Intersection 4	58	5	0	96

Note: SB = Southbound; LT = left-turn.

**Figure 4.** The key geometric and volume information associated with the study site.

Note: vph = vehicles per hour.

Study Site

Figure 4 shows the key geometric information and the input volume associated with the study site at I-270 @ MD 187 in Maryland for extensive analysis. The freeway mainline volume and hourly demand for all movements entering the target control area are shown in the figure, along with the number of lanes on the arterial links and the freeway segment. The eastbound on-ramp for metering control is colored in gray and the turning ratios onto the on-ramp are also shown. The minimum and maximum cycle lengths are 90 and 180 s, respectively. The model is solved with Gurobi 9 (32) on a Windows 10 desktop with an Intel Core i7-6700 processor and 16GB RAM. The computation times are less than 5 s.

Table 2 show the AF-ramp model's key output for the area-wide ramp control under the following scenarios of different volumes and ramp lengths:

- Scenario 1: the base-level volume as shown in Figure 4;
- Scenario 2: same as Scenario 1 but with an increase of 10% to all arterial volumes;
- Scenario 3: same as Scenario 1 but with an increase of 20% to all arterial volumes; and
- Scenario 4: same as Scenario 3 but with a shorter ramp length (from 792 ft to 500 ft).

Note that the optimal on-ramp metering green ratio, as expected, increases with the arterial's volume (i.e., from 0.38 for Scenario 1 to 0.47 for Scenario 3), confirming the AF-ramp model's unique feature to adjust the ramp metering rate, based not only on the available free-way capacity, but also on the on-ramp volume from its neighboring intersections. Also, note that the model will concurrently increase the ramp green ratio (from 0.38 to 0.47) and intersection's cycle length (90–150 s) to accommodate the 20% volume surge as in Scenario 3.

To prevent queue spillback on a short ramp as in Scenario 4, the proposed model with its embedded functions for capturing the interrelations between the ramp and arterial flows can concurrently generate a shorter cycle length and less green ratio to constrain the on-ramp's arriving flows. For instance, compared with Scenario 3, the cycle length in Scenario 4 is reduced from 150 s to 100 s, along with a slightly adjusted green ratio (from 0.42 to 0.41) for the left-turn movement to get onto the ramp.

In brief, the above results of numerical investigation clearly show that the AF-ramp model with its function for optimizing the cycle length concurrently with the ramp metering rate can indeed best use the capacity of local intersections and prevent any gridlock by overflows from the on-ramp queue spillback.

Table 3. Average Speed with Two Control Strategies under Scenarios 1 and 2

Location	P ₁	P ₂	P ₃	P ₄	P ₅
Scenario 1: Three-lane average speed (mph)					
No-RM	54.7	45.2	38.3	44.7	50.1
Proposed	56.6 (3.5%)	51.1 (13.1%)	46.6 (21.5%)	45.2 (1.1%)	50.2 (0.2%)
Scenario 1: Rightmost lane average speed (mph)					
No-RM	54.5	42.4	34.2	42.6	50.0
Proposed	56.6 (3.7%)	48.5 (14.4%)	42.8 (25.0%)	44.0 (3.3%)	50.2 (0.4%)
Scenario 2: Three-lane average speed (mph)					
No-RM	49.2	38.0	33.9	44.5	50.1
Proposed	53.3 (8.4%)	47.9 (26.1%)	40.4 (19.5%)	44.5 (0.1%)	50.1 (−0.1%)
Scenario 2: Rightmost lane average speed (mph)					
No-RM	48.9	35.0	28.6	42.0	50.0
Proposed	53.1 (8.4%)	45.2 (29.0%)	36.0 (25.7%)	43.2 (2.7%)	50.0 (−0.1%)

Note: RM = ramp metering. Percentages in the brackets indicate the improvement over the No-RM strategy.

Simulation Experiments

To evaluate the model's effectiveness with other MOEs, this study has further conducted simulation experiments with Scenarios 1 and 2 using VISSIM. The performance of the proposed model has been compared with the following two controls:

- no-RM control: no metering control and the arterial signal timing is calculated with Critical Lane Volume (CLV) and the coordination offsets are optimized with MAXBAND (33); and
- RM-only control: the ramp metering rate is set only to maximize the freeway throughput based on Equation 21, and the arterial signal timing plan is optimized independently as with the No-RM control.

The set of MOEs generated from the simulation includes: (1) average vehicle speed for all lanes and on the rightmost lane, collected at five locations (denoted as P₁ to P₅) shown in Figure 4; (2) completed trips on the freeway mainline over the one-hour control period; (3) average freeway mainline delay; (4) arterial's total throughput from the target control area (including all movements leaving the target control area shown in Figure 4); (5) average arterial through-movement delay; (6) network average delay; and (7) queue lengths on the on-ramp and arterial links. The results are obtained from 10 simulation runs with different random seeds.

Figure 5 shows the time-dependent on-ramp queue length with the AF-ramp model and the RM-only control under two scenarios. As expected, the RM-only control, without accounting for the arterial traffic, would rapidly increase the on-ramp queues and further overflow those vehicles to the upstream intersections about 1,600 ft away. In contrast, such on-ramp queue vehicles under the AF-ramp control are all constrained within

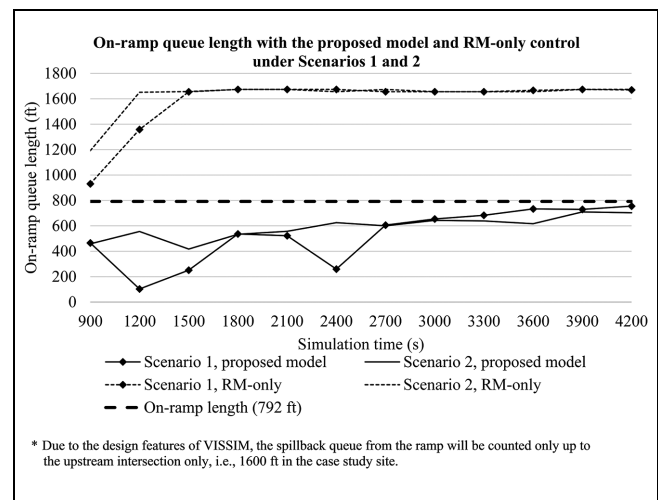


Figure 5. Evolution of on-ramp queue length with the proposed model and RM-only control.

Note: RM = ramp metering.

the ramp up to the end of the control period, due mainly to the higher metering rate designed to avoid on-ramp queue spillback and the coordinated operation of the arterial signals.

Note that since RM-only control will yield undesirably long queues to the arterial, the benefits analysis presented below for the developed AF-ramp model will focus on its resulting benefits using the No-RM control as the baseline for comparison. Tables 3 and 4 show the average speed of all lanes and on the rightmost lane, along with all other MOEs with these two control strategies under Scenarios 1 and 2. Figure 6 further shows the results from the same comparison but focuses on the time-dependent queue length on the arterial link, which is often plagued by the excessive queues in the vicinity of the freeway ramp.

Table 4. Related Measures of Effectiveness with Two Control Strategies under Scenarios 1 and 2

	Freeway mainline average delay (s)	Freeway mainline completed trips	Average arterial through delay (s)	Arterial throughput (vph)	Network average delay (s)
SCENARIO 1					
No-RM	32.17	5592	100.14	6180	70.29
Proposed	17.62 (45.2%)	5621 (0.5%)	76.63 (23.5%)	6193 (0.2%)	53.92 (23.3%)
SCENARIO 2					
No-RM	51.90	5522	105.54	6777	82.92
Proposed	29.15 (43.8%)	5591 (1.2%)	86.83 (17.7%)	6800 (0.3%)	61.97 (25.3%)

Note: vph = vehicles per hour; RM = ramp metering. Percentages in the brackets indicate the improvement over the No-RM strategy.

As shown in Table 3, the freeway segment upstream of the on-ramp, without ramp metering control, exhibits a significant speed drop, but the traffic flows will recover the speed when passing the ramp and entering the downstream segment. For example, under Scenario 1, the average speed progressively drops from its initial speed of 54.7 mph at the most upstream detection point to 38.3 mph right at the on-ramp merging area, and then back to 50.1 mph at the P_5 detection point. One can also detect the same spatial evolution pattern of the average speed for Scenario 2, but with a more pronounced drop because of the impact of higher ramp flows (i.e., from 49.2 mph to 33.9, and back to 50.1 mph). In both scenarios, the rightmost lane, as shown in Table 3, suffers the most impact from the ramp flows, reducing its speed from 54.5 mph to 34.2 mph in Scenario 1, and likewise from 48.9 mph to 28.6 mph in Scenario 2. Such a significant speed drop clearly justifies the need to implement ramp metering.

In contrast, under the proposed AF-ramp control, the freeway's average speed on the bottleneck segment increases from 45.2 mph to 51.1 mph at P_2 , and 38.3 mph to 46.6 mph at P_3 in Scenario 1, an average of 17.3% (i.e., 13.1% and 21.5%) improvement. As expected, the rightmost lane, generally benefiting more from an effective ramp metering control, exhibits the speed improvement of 14.4% and 25.0%, respectively, in Scenario 1, over the same detection points in the bottleneck area. In general, the magnitude of such improvement may increase with the ramp volume, as evidenced by the 29.0% and 25.7% speed improvement for the rightmost lane under Scenario 2 at the same data collection points.

Table 4 summarizes various MOEs for both the freeway and arterial with the AF-ramp model and under No-RM control, where the delay on the freeway mainline reduces by 45.2% and 43.8%, respectively under these two scenarios, attributed mainly to the AF-ramp control's function to prevent the formation of a local bottleneck by the on-ramp flows.

With respect to the widespread concern that freeway improvements under ramp metering will inevitably

generate negative impacts on local traffic, the results in Table 4 clearly show that the arterial's traffic conditions can concurrently benefit from the proposed control strategy. For example, the through movement's average delay exhibits a reduction of 23.5% and 17.7%, respectively, in Scenarios 1 and 2, because of the AF-ramp model's embedded progression design and its coordinated function between the metering rate and the intersection signal plans. In addition, the same arterial throughput under these two controls further indicates that the ramp control with the AF-ramp model will not have undesirable effects on the local traffic flows.

To ensure that the coordination between intersection signals and ramp metering control will not result in excessive queues on the arterial links, especially those accommodating vehicles turning to the ramp, this study has further analyzed the queue length evolution at all intersection approaches and confirmed that no links or turning bays have experienced traffic overflows under the AF-ramp control. For example, the queue evolution patterns for the northbound through movement at Intersection 3 and southbound left-turn traffic at Intersection 2, shown in Figure 6, clearly demonstrate that those arterial links connecting to the freeway ramp are likely to experience traffic gridlock and extend their queues to their upstream intersections under No-RM control. However, under the specially designed local progression and coordination with ramp metering control, both arterial links under AF-ramp can well constrain the resulting queues in a relatively stable pattern, and also within their designated space.

In brief, the above analysis results from both the numerical investigation and simulation evaluation have confirmed the developed AF-ramp model's effectiveness in concurrently improving traffic conditions on both the freeway and its neighboring arterial links, and most importantly, yielding no queue spillback on either the ramp or arterial links. With such an arterial-friendly ramp control system, traffic agencies responsible for operations of the freeway and local arterial can work together to contend with the freeway's local bottleneck

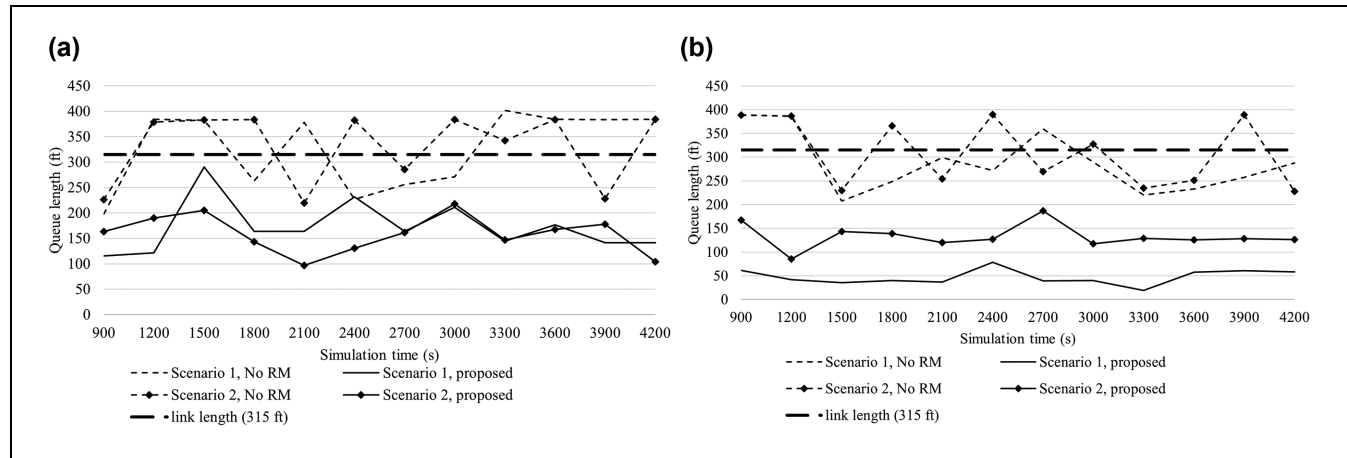


Figure 6. Time-dependent queue length on the arterial link with the proposed model and No-RM control under the two scenarios: (a) northbound through queue length at Intersection 3; and (b) southbound left-turn queue length at Intersection 2.

Note: RM = ramp metering.

because of high ramp volume, and also alleviate the negative impacts of ramp overflows on local traffic conditions.

Extension of the Proposed Model to Real-Time Operation

Note that ramp metering control strategies should in theory be designed for real-time traffic-responsive operations in response to the time-varying volumes on the freeway and nearby local arterials. The proposed AF-ramp system and its core functions can be ready for use in real-time operations if the responsible highway agencies have reliable sensor deployment and sufficient resources for real-time operations, monitoring, and maintenance. The alteration to the proposed formulations for real-time traffic-responsive operation should at least include a requirement to:

- replace the constant demand flows with predicted demand at both the freeway upstream segment and arterial boundary intersections based on reliable volume prediction methods;
- change the allowable maximum on-ramp queue length in Equation 8 to a time-dependent parameter to ensure that the on-ramp queue would not expand rapidly and occupy the entire on-ramp immediately after the activation of RM control;
- examine the discrepancy between the calculated and real-time detected queue length at the on-ramp and update the queue length constraint accordingly;
- include a detector surveillance system to activate the backup off-line plan when the detectors malfunction; and

- examine the discrepancy between the calculated and detected throughput at the on-ramp weaving area and update the related model parameters if needed.

We, however, recognized that the lack of sufficiently reliable sensors and the shortage of resources for maintenance and operations have limited most real-time control systems to operating at the demonstration level but not being used sustainably in practice. Therefore, this study presents an alternative as a transition from time-of-day pre-timed control to fully responsive real-time operations, based on the core logic of the proposed model. This alternative is also proposed in response to the actual concern in practice, because most arterial controllers for intersection signals in most states are not designed for adaptive operations, and mostly cannot change their signal plans as conveniently and frequently as for the local ramp signal. To extend the AF-ramp model from the time-of-day control to the real-time mode, one viable way to circumvent the demanding on-line computing requirements is to divide the control period as well as possible into a sufficient number of small time periods based on the day-to-day detected traffic patterns, and then monitor such time-of-day control with the information from real-time available traffic data.

As shown in Figure 7, traffic operators, in practice, can first execute the optimal control plan, computed off-line with the AF-ramp for each time period, and then proceed with real-time available traffic data and queue information. If the detected traffic information for either freeway or local arterials differs significantly and sustainably from the traffic data classified for that control period, one can then switch to a new control plan from the database that contains the set of off-line optimized

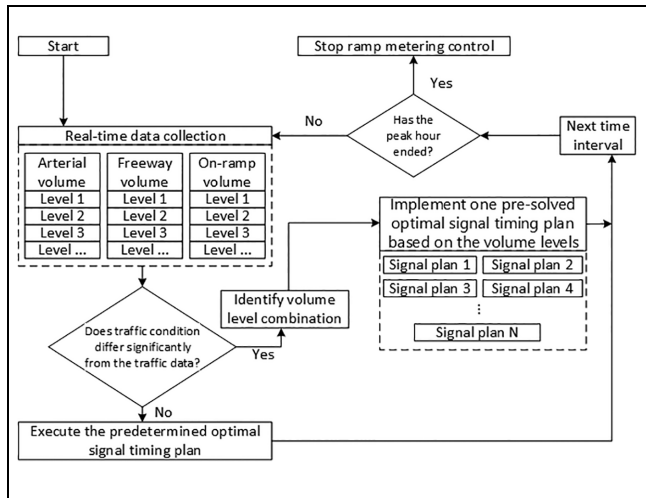


Figure 7. Real-time operation of arterial-friendly local ramp metering system.

control plans for all observed day-to-day historical traffic patterns.

Conceivably, such a real-time operating system extended from time-of-day off-line control does not require its controller to have high computing power and is sufficiently flexible for accommodating fluctuating traffic conditions and non-recurrent congestion because of special events or incidents. Note that to optimize such a system's performance in real-time operations, it should ideally also have one supplemental module that functions to inform the system with respect to the optimal timing to change the current control plan if it is justified to do so, and also the selection of new plans from the database to best respond to the newly detected traffic conditions.

Conclusion

This study has proposed an arterial-friendly local ramp metering control strategy to concurrently optimize the ramp metering rate and signal plans at those intersections feeding traffic to a freeway on-ramp. With the objective of maximizing the total throughput for both the freeway segment receiving the on-ramp flows and the connected arterial links within the control area, the proposed model can serve as an effective tool for responsible freeway and arterial traffic agencies to coordinate their operations with the mutual-benefit control plan.

More specifically, to ensure that the intersections on the local arterial would not suffer from on-ramp queue spillback, the maximum queue length, estimated with the arriving on-ramp volume and the optimized metering rate, has been constrained to be within the ramp length. On the other hand, the arterial's signal plan has also been designed with optimally coordinated offsets and phase

sequences to maximize the progression efficiency for both through and turning flows over intersections within the vicinity of the interchange.

The results of extensive numerical investigations have confirmed that the proposed model can best use the capacity of the freeway segment in the merging area and prevent any potential gridlock that results from the on-ramp queue spillback with the concurrently optimized intersection signal plan and ramp metering rate. The simulation studies have further demonstrated that the AF-ramp model can improve the traffic conditions on the freeway mainline near the on-ramp while avoiding both excessive ramp queues and arterial link overflows with a set of specially designed progression offsets.

As a transition from the time-of-day control to fully traffic-responsive operations and to minimize the required expertise and hardware requirements for real-time operations of the proposed system, this study has also presented a look-up table approach (similar to that used in Urban Traffic Control System 1.5) for the system to execute a timely update of its control plan when detecting significant variation in traffic conditions. Further studies along this line will include the extension of the proposed arterial-friendly model to coordinated ramp metering control in a traffic corridor. A more comprehensive structure for real-time traffic-responsive operation to benefit both freeway and arterial users will also be developed.

Acknowledgments

The support from Allison Hardt, Hua Xiang, Mohammed Raqib is greatly appreciated.

Author Contributions

The authors confirm contribution to the paper as follows: study conception and design: Yao Cheng, Gang-Len Chang; data collection: Yao Cheng; analysis and interpretation of results: Yao Cheng; draft manuscript preparation: Yao Cheng, Gang-Len Chang. All authors reviewed the results and approved the final version of the manuscript.

Declaration of Conflicting Interests

The author(s) declared no potential conflicts of interest with respect to the research, authorship, and/or publication of this article.

Funding

The author(s) disclosed receipt of the following financial support for the research, authorship, and/or publication of this article: This study is from the project, "Integration of Ramp Metering and Off-Ramp Progression" (Project No.: SP910B4B) sponsored by Maryland Department of Transportation State Highway Administration.

References

1. Wattleworth, J. A. *Peak-Period Analysis and Control of a Freeway System*. No. Hpr 1/4/. Texas Transportation Institute, College Station, TX, 1965.
2. Wang, J. J., and A. D. May. Computer Model for Optimal Freeway On-Ramp Control. *Highway Research Record: Journal of the Highway Research Board*, 1973. 469: 16–25.
3. Chen, C.-I., J. B. Cruz, Jr., and J. G. Paquet. Entrance Ramp Control for Travel-Rate Maximization in Expressways. *Transportation Research*, Vol. 8, No. 6, 1974, pp. 503–508.
4. Papageorgiou, M., H. Hadj-Salem, and J. M. Blosseville. ALINEA: A Local Feedback Control Law for On-Ramp Metering. *Transportation Research Record: Journal of the Transportation Research Board*, 1991. 1320: 58–67.
5. Papageorgiou, M., H. Hadj-Salem, and F. Middelham. ALINEA Local Ramp Metering: Summary of Field Results. *Transportation Research Record: Journal of the Transportation Research Board*, 1997. 1603: 90–98.
6. Smaragdis, E., and M. Papageorgiou. Series of New Local Ramp Metering Strategies: Emmanouil Smaragdis and Markos Papageorgiou. *Transportation Research Record: Journal of the Transportation Research Board*, 2003. 1856: 74–86.
7. Wang, Y., E. B. Kosmatopoulos, M. Papageorgiou, and I. Papamichail. Local Ramp Metering in the Presence of a Distant Downstream Bottleneck: Theoretical Analysis and Simulation Study. *IEEE Transactions on Intelligent Transportation Systems*, Vol. 15, No. 5, 2014, pp. 2024–2039.
8. Kachroo, P., K. Ozbay, and D. E. Grove. Isolated Ramp Metering Feedback Control Utilizing Mixed Sensitivity for Desired Mainline Density and the Ramp Queues. *Proc., ITSC 2001. 2001 IEEE Intelligent Transportation Systems*, Oakland, CA, IEEE, New York, 2001, pp. 631–636.
9. Zhang, H. M., and S. G. Ritchie. Freeway Ramp Metering using Artificial Neural Networks. *Transportation Research Part C: Emerging Technologies*, Vol. 5, No. 5, 1997, pp. 273–286.
10. Paesani, G. F. System Wide Adaptive Ramp Metering in Southern California. *Proc., ITS America 7th Annual Meeting and Exposition: Merging the Transportation and Communications Revolutions*, Washington, D.C., 1997.
11. Papamichail, I., M. Papageorgiou, V. Vong, and J. Gaffney. Heuristic Ramp-Metering Coordination Strategy Implemented at Monash Freeway, Australia. *Transportation Research Record: Journal of the Transportation Research Board*, 2010. 2178: 10–20.
12. Papageorgiou, M., J. M. Blosseville, and H. Haj-Salem. Modelling and Real-Time Control of Traffic Flow on the Southern Part of Boulevard Périphérique in Paris: Part II: Coordinated On-Ramp Metering. *Transportation Research Part A: General*, Vol. 24, No. 5, 1990, pp. 361–370.
13. Wang, Y., K. A. Perrine, and Y. Lao. *Developing an Area-Wide System for Coordinated Ramp Meter Control*. No. TNW2008-11. Transportation Northwest (Organization), Seattle, WA, 2008.
14. Lipp, L. E., L. J. Corcoran, and G. A. Hickman. Benefits of Central Computer Control for Denver Ramp-Metering System. *Transportation Research Record: Journal of the Transportation Research Board*, 1991. 1320: 3–6.
15. Liu, J. C. S., J. L. Kim, Y. Chen, Y. Hao, S. Lee, T. Kim, and M. Thomadakis. *An Advanced Real-Time Ramp Metering System (ARMS): The System Concept*. Texas Transportation Institute, Austin, TX, Vol. 1232, No. 24, 1994.
16. Shaaban, K., M. A. Khan, and R. Hamila. Literature Review of Advancements in Adaptive Ramp Metering. *Procedia Computer Science*, Vol. 83, 2016, pp. 203–211.
17. Zhang, M., T. Kim, X. Nie, W. Jin, L. Chu, and W. Recker. *Evaluation of On-Ramp Control Algorithms*. Research Reports. University of California, Berkeley, 2001.
18. Kattan, L., and M. S. Saidi. *Design and Evaluation of Adaptive Coordinated Ramp Control Strategies on Deerfoot Trail using Paramics Microsimulation*. Final Report. University of Calgary, Alberta, Canada, 2011.
19. Gordon, R. L. Algorithm for Controlling Spillback from Ramp Meters. *Transportation Research Record: Journal of the Transportation Research Board*, 1996. 1554: 162–171.
20. Sun, X., and R. Horowitz. A Localized Switching Ramp-Metering Controller with a Queue Length Regulator for Congested Freeways. *Proc., 2005 American Control Conference*, Portland, OR, IEEE, New York, 2005, pp. 2141–2146.
21. Su, D., X. Y. Lu, R. Horowitz, and Z. Wang. Coordinated Ramp Metering and Intersection Signal Control. *International Journal of Transportation Science and Technology*, Vol. 3, No. 2, 2014, pp. 179–192.
22. Lertworawanich, P., and L. Elefteriadou. Capacity Estimations for Type B Weaving Areas Based on Gap Acceptance. *Transportation Research Record: Journal of the Transportation Research Board*, 2001. 1776: 24–34.
23. Won, M. *Development of a Traffic Incident Management Support System*. Doctoral dissertation. University of Maryland, College Park, MD, 2019.
24. Roess, R. P., and J. M. Ulerio. Capacity of Freeway Weaving Segments. *Transportation Research Record: Journal of the Transportation Research Board*, 2009. 2130: 34–41.
25. Rakha, H., and Y. Zhang. Analytical Procedures for Estimating Capacity of Freeway Weaving, Merge, and Diverge Sections. *Journal of Transportation Engineering*, Vol. 132, No. 8, 2006, pp. 618–628.
26. Lertworawanich, P., and L. Elefteriadou. A Methodology for Estimating Capacity at Ramp Weaves Based on Gap Acceptance and Linear Optimization. *Transportation Research Part B: Methodological*, Vol. 37, No. 5, 2003, pp. 459–483.
27. Kwon, E. *Estimation of the Capacity in Freeway Weaving Areas for Traffic Management and Operations*. Minnesota Department of Transportation, Retrieved from the University of Minnesota Digital Conservancy, 1999. <http://hdl.handle.net/11299/152959>.
28. van Beinum, A., H. Farah, F. Wegman, and S. Hoogendoorn. Driving Behaviour at Motorway Ramps and Weaving Segments Based on Empirical Trajectory Data. *Transportation Research Part C: Emerging Technologies*, Vol. 92, 2018, pp. 426–441.
29. Zheng, Z., S. Ahn, D. Chen, and J. Laval. The Effects of Lane-Changing on the Immediate Follower: Anticipation,

- Relaxation, and Change in Driver Characteristics. *Transportation Research Part C: Emerging Technologies*, Vol. 26, 2013, pp. 367–379.
30. Zheng, Z., S. Ahn, D. Chen, and J. Laval. Freeway Traffic Oscillations: Microscopic Analysis of Formations and Propagations using Wavelet Transform. *Procedia-Social and Behavioral Sciences*, Vol. 17, 2011, pp. 702–716.
31. Chen, Y., Y. Cheng, and G. Chang. Design of Multi-Path Traffic Progression for Congested Arterials with Connected Local Progression Bands. Presented at 99th Annual Meeting of the Transportation Research Board, Washington, D.C., 2020.
32. GUROBI OPTIMIZATION. INC. *Gurobi Optimizer Reference Manual*. Gurobi Optimization, LLC, Houston, TX, 2015. <http://www.gurobi.com>, p.29. 2014.
33. Little, J. D., M. D. Kelson, and N. H. Gartner. *MAX-BAND: A Versatile Program for Setting Signals on Arteries and Triangular Networks*. Federal Highway Administration, Washington, D.C., 1981.